

LETTER • **OPEN ACCESS**

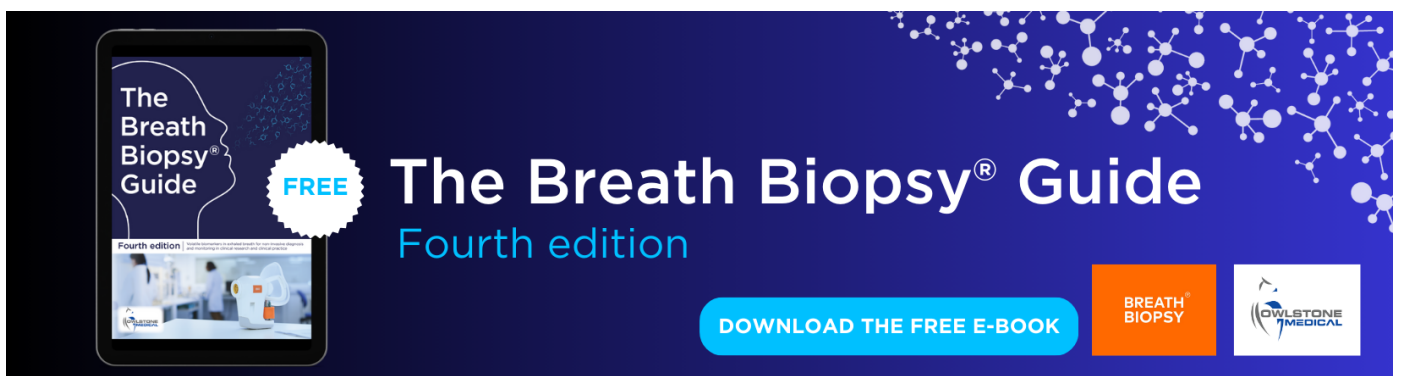
Processes explaining increased ocean dynamic sea level in the North Sea in CMIP6

To cite this article: Franka Jesse *et al* 2024 *Environ. Res. Lett.* **19** 044060

View the [article online](#) for updates and enhancements.

You may also like

- [Comparison of bio-physical marine products from SeaWiFS, MODIS and a bio-optical model with *in situ* measurements from Northern European waters](#)
D Blondeau-Patissier, G H Tilstone, V Martinez-Vicente et al.
- [The exceptional influence of storm 'Xaver' on design water levels in the German Bight](#)
Sönke Dangendorf, Arne Arns, Joaquim G Pinto et al.
- [Constructing scenarios of regional sea level change using global temperature pathways](#)
Hylke de Vries, Caroline Katsman and Sybren Drijfhout



The Breath Biopsy® Guide
Fourth edition

FREE

DOWNLOAD THE FREE E-BOOK

BREATH BIOPSY

OWLSTONE MEDICAL

ENVIRONMENTAL RESEARCH
LETTERS

LETTER

Processes explaining increased ocean dynamic sea level in the North Sea in CMIP6

OPEN ACCESS

RECEIVED
28 June 2023REVISED
28 February 2024ACCEPTED FOR PUBLICATION
14 March 2024PUBLISHED
3 April 2024

Original Content from
this work may be used
under the terms of the
[Creative Commons
Attribution 4.0 licence](#).

Any further distribution
of this work must
maintain attribution to
the author(s) and the title
of the work, journal
citation and DOI.

Franka Jesse^{1,2,*} , Dewi Le Bars¹  and Sybren Drijfhout^{1,2}¹ Royal Netherlands Meteorological Institute (KNMI), De Bilt, The Netherlands² Institute for Marine and Atmospheric Research Utrecht, Utrecht University, Utrecht, The Netherlands

* Author to whom any correspondence should be addressed.

E-mail: t.f.jesse@uu.nl**Keywords:** sea level, ocean dynamics, North Sea, AMOC, mixed layer depth, CMIP5, CMIP6Supplementary material for this article is available [online](#)**Abstract**

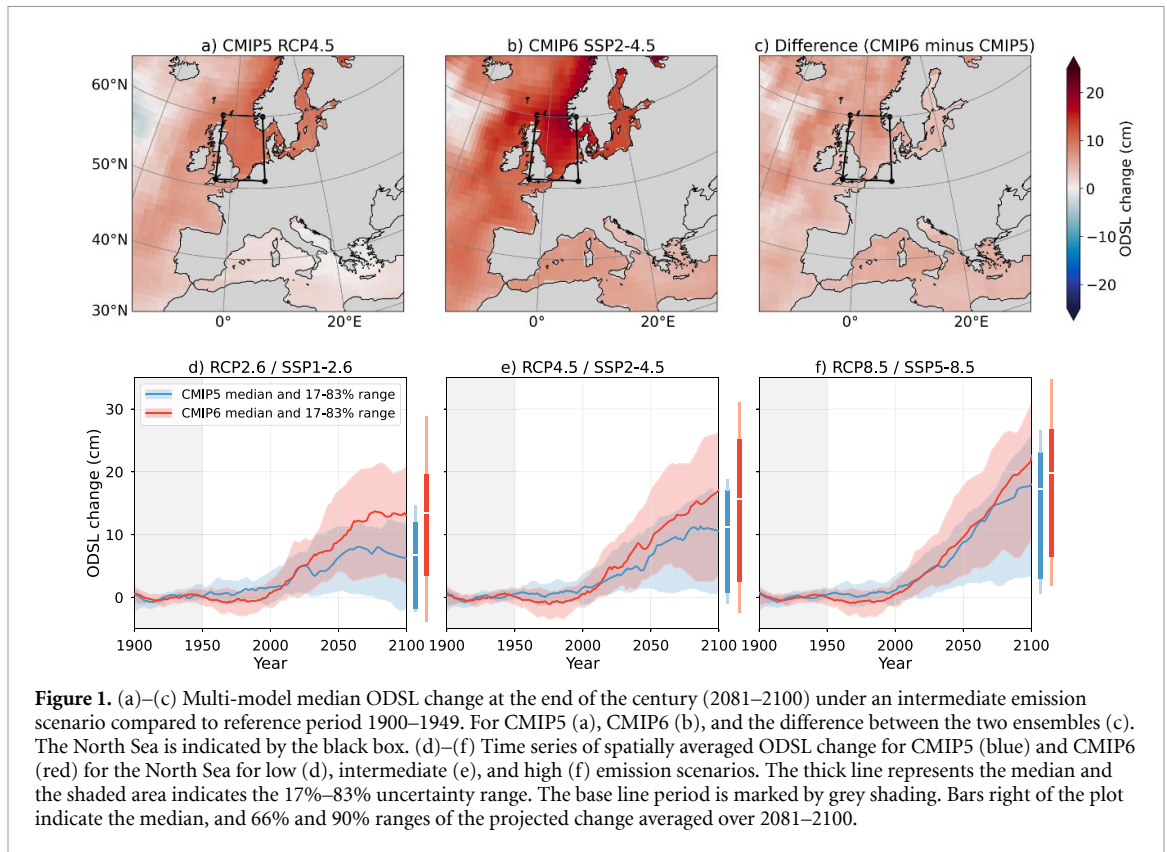
Ocean dynamic sea level (ODSL) is expected to be one of the major contributors to sea level rise in the North Sea during the 21st century. This component is defined as the spatial sea level anomaly due to ocean currents, wind stresses and local thermosteric and halosteric effects. Climate models from CMIP5 and CMIP6 show a large spread, as well as an increase between CMIP5 and CMIP6 North Sea ODSL projections. In this study, we apply linear regression models on CMIP5 and CMIP6 data to get a better understanding of the processes that influence ODSL change in the North Sea. We find that neither global surface air temperature nor global mean thermosteric sea level can reproduce ODSL projections based on a linear relation in CMIP6, whereas this was the case for CMIP5. Including the strength of the Atlantic meridional overturning circulation (AMOC) as an additional predictor enables us to reproduce long-term changes in ODSL for both ensembles. The sensitivity to the AMOC increased in CMIP6, which points to a difference in model dynamics between CMIP5 and CMIP6, and a more important role of the deep ocean. To investigate this further, we analyse mixed layer depth data in the North Atlantic. We find that models with a relatively deep mixed layer in the Greenland Sea over the period 1985–2004, project larger rise in ODSL in the North Sea for both CMIP5 and CMIP6. This implies that the location of deep water formation in the North Atlantic potentially influences ODSL in the North Sea. The number of these models increased from CMIP5 to CMIP6, again pointing to a different sensitivity to larger scale processes, potentially explaining the difference between the two ensembles.

1. Introduction

Sea level rise is one of the main consequences of global warming. The rise of global mean sea level has accelerated over the past decades due to thermal expansion of sea water and an increased mass loss of land ice (Dangendorf *et al* 2019). Projections show that global mean sea level will continue to rise during the 21st century as a consequence of anthropogenic forcing (Slangen *et al* 2016, Oppenheimer *et al* 2019, Fox-Kemper *et al* 2021). The rise of sea level has a broad socio-economic and environmental impact on coastal communities and low-lying countries (Hinkel *et al* 2014). In this study, we focus on the North Sea area, where millions of citizens live within 50 km from

the coastline (Vousdoukas *et al* 2020). As sea level rise will have a large impact in this area, it is of significant importance to provide policymakers with reliable projections that can serve as the basis for implementing adequate adaptation measures (Hinkel *et al* 2019).

Regional differences in sea level projections arise mainly from three processes: ocean dynamics, rotational and gravitational effects, and vertical land motion. In the North Sea, the sea level rise due to ocean dynamics, hereafter referred to as ocean dynamic sea level (ODSL), is one of the major contributors to total sea level rise during the 21st century (de Vries *et al* 2014). ODSL is defined as the sea level deviation from the geoid, with the inverse barometer correction applied (Gregory *et al* 2019). This



means that it reflects the sea level anomaly due to local thermosteric and halosteric effects, ocean currents and wind stresses (Gill and Niller 1973, Gregory *et al* 2016).

The primary tools to construct ODSL projections are atmosphere–ocean general circulation models. In this study, we analyse ODSL simulations from the latest two phases from the Coupled Model Intercomparison Project (CMIP5 and CMIP6) forced by three different emission scenarios (Jesse 2022).

Figure 1 shows a comparison of the two ensembles. For the intermediate emission scenario, the median ODSL change at the end of the century in CMIP5 (panel (a)) has a similar pattern as in CMIP6 (panel (b)). The difference between CMIP5 and CMIP6 (panel (c)) is similar to the sea level change patterns themselves, suggesting an amplification of the CMIP5 pattern in CMIP6, in line with findings reported by Lyu *et al* (2020). The North Sea, indicated by the black box, is one of the regions that show larger increase in ODSL, together with the area along the Norwegian coast and North and West of the British Isles. The same is found for the lower and higher emission scenarios. The time series for North Sea ODSL presented in panels (d)–(f) in figure 1 show a slight positive trend in the CMIP5 models for all scenarios during the 20th century, followed by a faster rise between 2000–2075 and a drop after 2075 for the low and intermediate emission scenarios. The CMIP6 ensemble shows no rise in ODSL during the

20th century, followed by a fast rise starting around 1990. For the low and intermediate scenarios, the rise slows down in 2060. For all three scenarios, the median end-of-the-century ODSL change is larger in CMIP6. Furthermore, for the low emission scenario, the end-of-the-century median of CMIP6 exceeds the 66% range of CMIP5. While AR6 (section 9.2.4.2, Fox-Kemper *et al* (2021)) states that the spread is similar in CMIP6 and CMIP5, our analysis shows that this is not the case for the North Sea. For each scenario, the spread in CMIP6 is larger and extends to higher values of ODSL change. To test whether the difference between the two ensembles is significant, we performed a Welch's *t*-test with the null hypothesis that the two ensembles have the same mean ODSL change at the end of the century. This null hypothesis is rejected for different reference periods and scenarios except for RCP8.5/SSP5–8.5 with the reference period 1900–1949 (supplementary material A, table A1).

The main objective of this study is to find out which processes can be related to ODSL change in the North Sea, and how they relate to the difference between CMIP5 and CMIP6. Inspired by earlier work (Perrette *et al* 2013, Bilbao *et al* 2015, Palmer *et al* 2020, Harrison *et al* 2021, Yuan and Kopp 2021), we investigate this with linear regression models using three explanatory variables: global mean surface air temperature (GSAT), global mean thermosteric sea level (GMTSL), and the strength

of the Atlantic meridional overturning circulation (AMOC). The importance of the latter for ODSL in the North Atlantic has been indicated in several studies (Katsman *et al* 2008, Bouttes *et al* 2014, Chen *et al* 2019, Lyu *et al* 2020). Next to the regression analysis, we explore whether the location of deep convection in the North Atlantic has an influence on ODSL projections in the North Sea.

2. Data

In this study, we analyse yearly averaged model output from a total of 30 CMIP5 models and 38 CMIP6 models. The complete list of models can be found in the supplementary material B, tables B1 and B2. Future scenarios are reflected by representative concentration pathways (RCPs) in CMIP5 as defined by Van Vuuren *et al* (2011), and by shared socioeconomic pathways (SSPs) in CMIP6 as defined by O'Neill *et al* (2014). In this study, three different scenarios are analysed: low radiative forcing (RCP2.6 / SSP1-2.6), intermediate radiative forcing (RCP4.5 / SSP2-4.5), and high radiative forcing (RCP8.5 / SSP5-8.5). We set the reference period for all variables to 1900–1949. One exception is made for the mixed layer depth (MLD) data, which is used as a proxy for the location of deep convection. For this variable, we are interested in the locations with a deep mixed layer during the late historical period and how they compare between different models. Therefore, we use the average MLD over the period 1985–2004. Below, we provide more information about the individual climate variables.

Simulations for ODSL are directly available as 'zos' in the CMIP5 and CMIP6 databases. Since the models do not discretise the ocean on identical grids, the data is regridded to the same $1.0^\circ \times 1.0^\circ$ grid. The pre-industrial control run is used to correct for the linear drift in each model's historical and future scenario simulations (Hobbs *et al* 2016) and the global mean is removed (Gregory *et al* 2019). ODSL in the North Sea is obtained by taking the spatial average over the region indicated by the black box in panels (a)–(c) of figure 1, spanning the area $51.5^\circ \text{ N} - 59.5^\circ \text{ N}$, $3.5^\circ \text{ W} - 7.5^\circ \text{ E}$. GSAT is obtained from computing the global mean of the CMIP variable 'tas'. GMTSL is given by the CMIP variable 'zostoga'. As is the case for zos, the linear drift in zostoga is removed using the piControl runs.

As a proxy for the AMOC strength we use the overturning mass stream function, given by 'msftmyz' in CMIP5, and by 'msftmz' (meridional direction) or 'msftyz' (y -direction) in CMIP6. For CMIP6, some models provide data for both variables msftmz and msftyz. In those cases, msftmz is used. No drift correction is performed for these variables. In the preparatory phase of this study, we considered the stream function at latitude 35° N and 26° N because these latitudes are often used as a proxy for the AMOC

strength (McCarthy *et al* 2020, Le Bras *et al* 2023). In the remainder of this article, we only show the results for latitude 35° N , since this turns out to be a better predictor in our regression analysis. The stream function with unit kg s^{-1} is divided by the average density of ocean water, $\rho = 1026 \text{ kg m}^{-3}$, and multiplied by 10^{-6} to obtain the AMOC strength in Sverdrups (Sv). Relatively few models that provide ODSL data, have one of these AMOC variables directly available. To expand the number of models we can use, we compute the AMOC for other models by integrating the meridional velocity, given by variable 'vo', at the same latitude of 35° N .

Lastly, we use MLD data, available as 'mldotst' in the CMIP database. Again, the number of models providing this data is limited. Therefore, we also use data from Heuzé (2021), where MLD is computed using monthly values for temperature and salinity. The MLD data is regridded to the same $1.0^\circ \times 1.0^\circ$ grid.

3. Methods

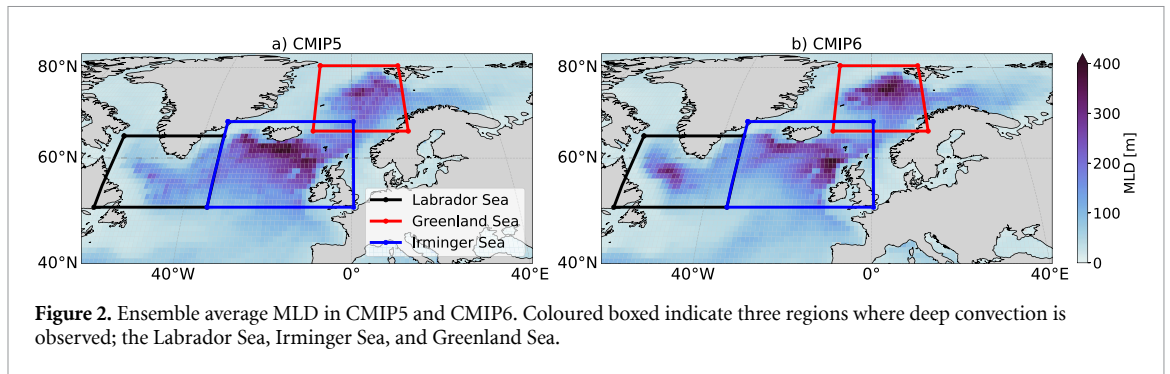
3.1. Linear regression models

The first predictor we consider is GSAT. This choice is motivated by the fact that ODSL is affected by changes in temperature and salinity in the ocean, which are themselves affected by changes in (among others) surface fluxes of heat (Lowe and Gregory 2006, Bouttes and Gregory 2014).

A second possible predictor is GMTSL. This variable depends on the interior redistribution of heat and therefore on the three-dimensional temperature field within the ocean. It thus reacts on different time scales than GSAT. Palmer *et al* (2020) present a set of local sea level projections based on the linear relation between ODSL and GMTSL in CMIP5 models. Moreover, the linear relation between these two variables is used by AR6 to correct ODSL from CMIP6 models (Kopp *et al* 2023).

Third, we take the AMOC as a predictor as several studies point to its importance for ODSL in the North Atlantic. Katsman *et al* (2008) found that a significant reduction of the AMOC correlated with larger steric sea level in the eastern North Atlantic using CMIP3 models. Chen *et al* (2019) found that the large uncertainty in CMIP5 ODSL projections in the North Atlantic is connected to the uncertainty in the change of the AMOC, and Lyu *et al* (2020) find that the larger ODSL change in the North Atlantic in CMIP6 is associated with a larger weakening of the AMOC.

The interannual variability in ODSL is relatively large, mainly due to wind effects. Our interest is however in the longer-term change in ODSL. Therefore, we exclude the short-term variability by applying a locally weighted scatterplot smoothing (LOWESS) filter to all variables included in the regression analysis (Cleveland and Devlin 1988). In this study, a window



size of 25 years is used in order to smooth the inter-annual variability out. Furthermore, we concatenate the historical time series from 1900 on with the available scenario runs. The regression analysis is then performed on the smoothed, concatenated time series to obtain scenario-independent regression coefficients between ODSL and the explanatory variables for each model.

We use a multilinear regression model given by

$$\text{ODSL}(t) = \alpha + \beta_1 x_1(t) + \beta_2 x_2(t) + \epsilon(t), \quad (1)$$

where α is the offset, x_1 and x_2 are the predictor variables, β_1 and β_2 are the regression coefficients, and ϵ is a time dependent error term. The maximum number of predictor variables is limited to two in order to avoid overfitting. We perform the regression analysis on all possible combinations of the predictor variables, and on the single variables (same as equation (1) but omitting the terms with subscript 2). As an additional validation measure, a LASSO regression is conducted to ascertain the most meaningful combinations of predictor variables (Tibshirani 1996). To evaluate and compare the performance of the different combinations of predictor variables in the regression model, we compute the root mean squared error (RMSE) of each linear fit.

Besides the three explanatory variables listed above (GSAT, GMTSL, and AMOC), we included zonal and meridional surface wind as regressors to investigate the potential influence of long-term wind effects on ODSL changes. Our regression analysis, however, indicated that surface winds are not an effective predictor of ODSL in the North Sea.

3.2. Deep ocean convection

Another process that could possibly influence local sea level is the location of deep convection. In this process, layers of water are mixed by gravitational instability after the surface layer loses buoyancy due to atmospheric cooling. It plays an important role in the formation of deep and intermediate water, and in the large-scale thermohaline circulation (Killworth 1983). Locations at which deep convection occurs are characterised by a deep mixed layer. In the North

Atlantic, this is observed south of Greenland in the Labrador Sea and Irminger Sea, and east of Greenland in the Greenland Sea (Killworth 1983, Heuzé 2017). To investigate whether the location of convection influences ODSL in the North Sea, we analyse the MLD data for the historic period 1985–2004. We focus on this period because a large number of models provide data for it, and considering the historic period gives an indication of the difference in deep ocean dynamics between models.

The ensemble averages of CMIP5 and CMIP6 (figure 2) show a deeper MLD in the three aforementioned regions, indicated by the coloured boxes. We categorise the individual models based on two conditions. First, we label them based on the region in which they show the deepest average MLD. Second, we categorise the models based on whether their average MLD in one of these regions exceeds the threshold of 170 m. This threshold is chosen since it splits both CMIP ensembles in similar-sized groups for the different regions. We use the same threshold for CMIP5 and CMIP6 to be able to compare the two ensembles. The number of models in the different categories is presented in table 1. To explore the effect of deep convection on North Sea ODSL, we analyse the differences in ODSL projections between the different categories.

4. Results and discussion

4.1. Regression models

In this section, we analyse the results of, and the difference between, the regression models for CMIP5 and CMIP6, computed for the concatenated time series. The ensemble average of the RMSE, and regression coefficients β_1 and β_2 are presented in table 2. We find that the RMSE increased between CMIP5 and CMIP6 for all regression models. Three models are discussed in more detail below.

The largest difference in RMSE, and therefore performance of the regression model, is found for the model using GSAT as a single regressor. The ensemble mean β_1 increased in CMIP6, as well as the spread in this coefficient (figure 3(c)). The time series of the ensemble-averaged regression model (figures 3(a)

Table 1. Number of CMIP5 and CMIP6 models in different MLD categories. In total, 24 CMIP5, and 35 CMIP6 models provide data for both MLD and ODSL. The first three rows display the number of models that show deepest MLD in the corresponding region, where Greenland Sea is denoted by GS, Irminger Sea by IS, and Labrador Sea by LS. The bottom three rows indicate the number of models exceeding the threshold of 170 meters in these regions.

Category	# CMIP5 models	# CMIP6 models
LS	4	9
GS	7	19
IS	13	7
LS _{≥170m}	7	11
GS _{≥170m}	12	19
IS _{≥170m}	17	12

Table 2. Ensemble mean RMSE and regression coefficients (β_1, β_2) for linear regression model: $ODSL(t) = \alpha + \beta_1 x_1(t) + \beta_2 x_2(t) + \epsilon(t)$, using different predictor variables (x_1, x_2). The linear regression is computed for the concatenated time series of the historical run and the available emission scenarios. Units of the scenario-independent regression coefficients depend on the predictor variable.

x_1	x_2	CMIP5			CMIP6		
		RMSE	β_1	β_2	RMSE	β_1	β_2
GSAT		3.10	3.62		10.19	4.58	
GMTSL		2.82	0.54		7.17	0.87	
AMOC35		5.43	-2.44		7.12	-2.11	
GSAT	GMTSL	2.36	2.08	0.29	6.25	1.66	0.62
GSAT	AMOC35	2.58	2.75	-0.64	4.01	1.93	-1.29
GMTSL	AMOC35	2.32	0.40	-0.82	4.42	0.41	-1.37

and (b)) show that this simple linear model is able to predict ODSL changes well for CMIP5 in all emission scenarios. For CMIP6, however, the regression model overestimates ODSL between 1960–2010. Furthermore, we see that the ODSL change is underestimated at the end of the 21st century for both SSP1-2.6 and SSP2-4.5. For SSP5-8.5, we see that the regression model overestimates the ODSL change at the end of the century. To investigate this further, we compute the linear regression for the individual scenarios (supplementary material C). For CMIP5, the scenario dependent regression coefficients hardly vary, whereas for CMIP6 they do, with the strongest sensitivity to GSAT in the low emission scenario and the weakest sensitivity in the high emission scenario. All together, these results state a clear difference between the two ensembles; namely that the linear relation between GSAT and ODSL in the North Sea does not hold in CMIP6, while it did in CMIP5.

The second model using GMTSL as a single regressor also shows a big increase in the ensemble-average RMSE between CMIP5 and CMIP6. For CMIP5 (figure 4(a)), the time series show that this regression model is able to capture most long-term changes in ODSL. Only at the end of the 21st century it overestimates the model output slightly. For CMIP6 (figure 4(b)), however, the drop around 1960 is again not captured by the linear relation. Furthermore, ODSL is underestimated between 2040 and 2080 in both SSP1-2.6 and SSP2-4.5. For the higher emission scenario, the regression model overestimates the end-of-the-century ODSL change. The

histogram of the regression coefficients (figure 4(c)) indicates that most models show a positive correlation between ODSL and GMTSL. An increase in dependence on GMTSL is seen in CMIP6, whereas the spread slightly decreased. Note that the linear relation between GMTSL and ODSL was used by Palmer *et al* (2020) to compute local sea level projections from CMIP5 global mean steric sea level. Here, we show that this linear relation is not able to reproduce all long-term variability in ODSL in the North Sea for the CMIP6 ensemble. Moreover, given the overestimation of the trend in ODSL at the end of the century, it is recommended not to use this linear relation for North Sea ODSL projections beyond 2100. This caution is especially relevant if GMTSL continues to rise exponentially, as this would lead to an overestimation of ODSL in the North Sea.

For CMIP6, the multilinear regression models using AMOC as an additional predictor perform best, based on their average RMSE (bottom two rows of table 2). For CMIP5, including the AMOC also reduces the RMSE with respect to the single predictor regression models. To verify these combinations of predictors, we carry out a LASSO regression. This regression method helps to select the relevant predictors and reduces overfitting. For models with data available for all three regressors, the LASSO regression indicates that the combination of GMTSL and AMOC is favoured by slightly more models compared to GSAT and AMOC. Both combinations lead to similar conclusions, indicating that there is something specific about the AMOC that

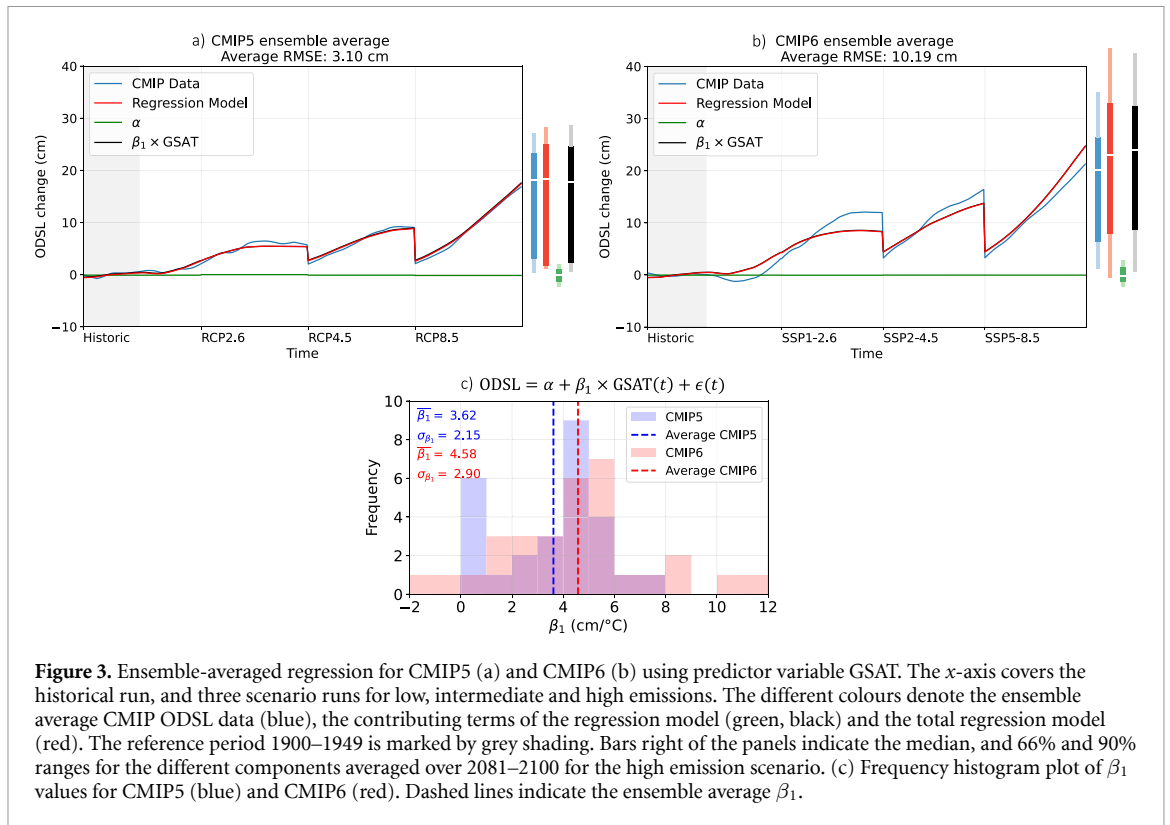


Figure 3. Ensemble-averaged regression for CMIP5 (a) and CMIP6 (b) using predictor variable GSAT. The x-axis covers the historical run, and three scenario runs for low, intermediate and high emissions. The different colours denote the ensemble average CMIP ODSL data (blue), the contributing terms of the regression model (green, black) and the total regression model (red). The reference period 1900–1949 is marked by grey shading. Bars right of the panels indicate the median, and 66% and 90% ranges for the different components averaged over 2081–2100 for the high emission scenario. (c) Frequency histogram plot of β_1 values for CMIP5 (blue) and CMIP6 (red). Dashed lines indicate the ensemble average β_1 .

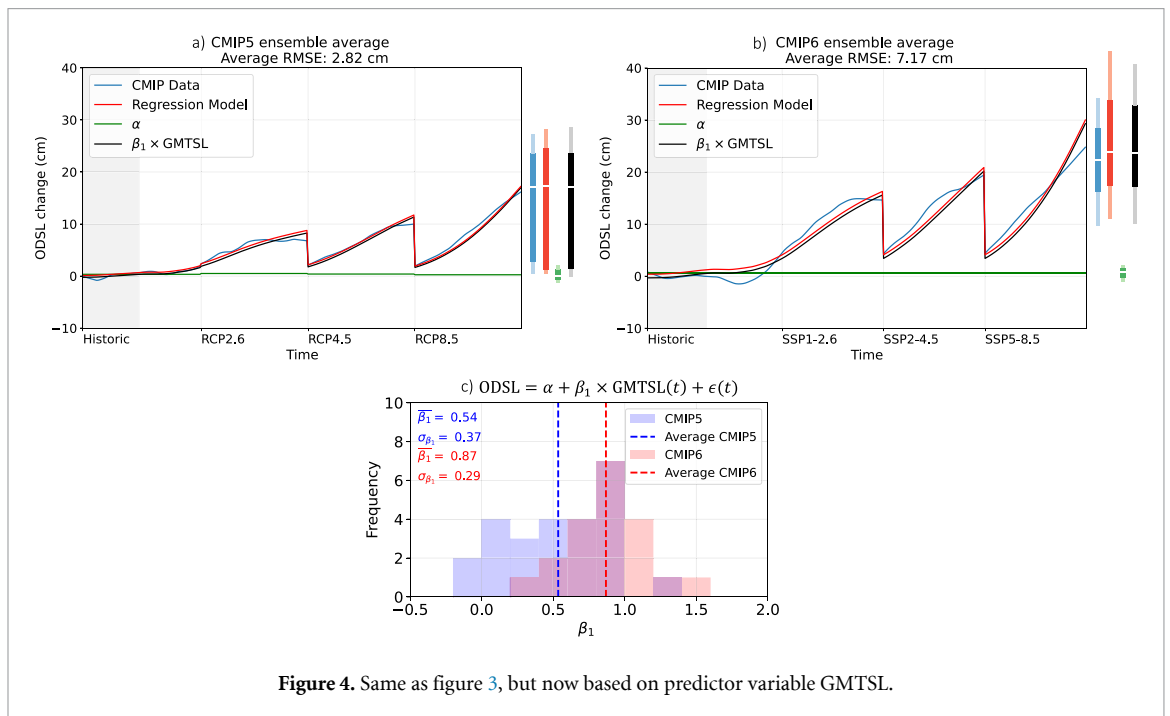


Figure 4. Same as figure 3, but now based on predictor variable GMTSL.

has an effect on ODSL which is not captured by GSAT nor GMTSL. This likely stems from the fact that the AMOC redistributes heat and salt within the Atlantic, whereas the other two variables merely reflect the global warming of the earth. In the following paragraph, we present results obtained from the regression model using the combination of GSAT and AMOC as predictor variables. First, because more

models have data available for this set of predictors. Second, using GSAT and AMOC allows us to investigate to what extent the increased climate sensitivity in CMIP6, reflected by a more substantial increase in GSAT (Forster *et al* 2020), explains the difference in ODSL change between CMIP5 and CMIP6. The results for the combination of GMTSL and AMOC can be found in supplementary material D, figure D3.

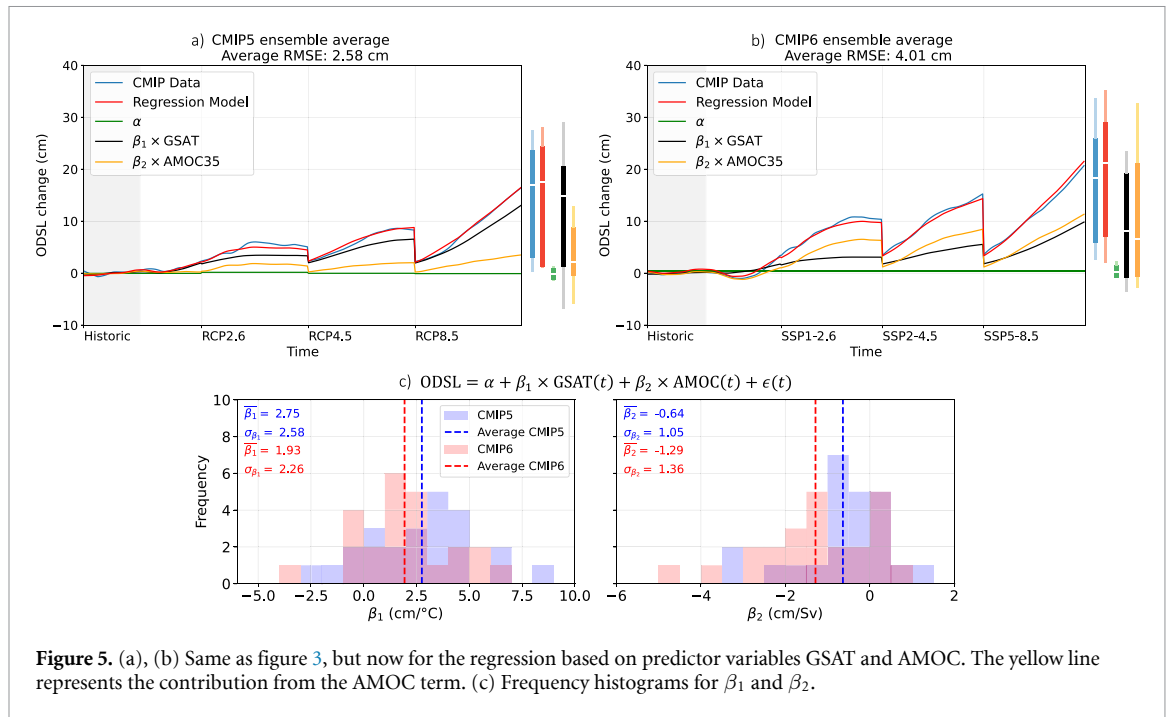


Figure 5. (a), (b) Same as figure 3, but now for the regression based on predictor variables GSAT and AMOC. The yellow line represents the contribution from the AMOC term. (c) Frequency histograms for β_1 and β_2 .

The time series in figure 5 show that the regression model using GSAT and AMOC is able to predict the end-of-the-century ODSL well for both CMIP5 and CMIP6. It captures most variability through the studied period. For instance, the drop in ODSL in CMIP6 around 1960 is explained by this regression model, as well as the flattening of the blue curve at the end of the century in the lower emission scenario (figure 5(b)). Upon comparing the uncertainty bars for CMIP6 with those in figures 3(b) and 4(b), particularly considering the 66% range, we find that this regression model outperforms the other regression models in reproducing end-of-the-century ODSL changes in the high emission scenario. One notable difference between the two ensembles is that the contribution from the AMOC term is substantially larger in CMIP6. This difference between CMIP5 and CMIP6 is also clear from the distributions of the regression coefficients (figure 5(c)). The dependence on GSAT is primarily positive, and a slightly smaller average β_1 is found for the CMIP6 ensemble. For the AMOC dependence, most models show a negative value for β_2 . Moreover, we find that the sensitivity to a change in AMOC increased in CMIP6.

We can use this linear model to assess the extent to which the difference in ODSL between CMIP5 and CMIP6 can be attributed to the difference in GSAT. We do this by computing corrected time series for CMIP6, in which we adjust the GSAT input to match the values from CMIP5. The details on these computations are given in supplementary material E. For the end of the century, this would reduce the difference between the two ensembles by 14.0%, 16.4%, and 16.0% for the low, intermediate and high emission

scenarios, respectively. This is, however, a small part of the total difference, indicating that the major part of the change is due to an increased sensitivity to AMOC changes versus decreased sensitivity to GSAT changes in CMIP6.

Time series of the other three regression models can be found in supplementary material D. The physical interpretation of the regression models using one single predictor variable is more straightforward than that of the models using two predictor variables. In general, we find a positive correlation between ODSL and GSAT, and ODSL and GMTSL. We find a negative correlation between AMOC and ODSL. However, none of these single predictor variable regression models does a good job at reproducing the long-term changes in ODSL. Therefore, we turn to the more complicated models with two predictor variables. We find that including AMOC as an additional predictor variable improves the predictive power, especially for CMIP6. However, the two predictor variables, AMOC and GSAT, are correlated with each other (supplementary material F). This so-called collinearity does not affect the predictive power of the regression model, but we do have to be careful with interpreting the results. To investigate the sensitivity, we repeated the analysis of this regression model for the original time series without smoothing and the time series smoothed with a window of 10 years instead of 25. In those two cases, we again see that the contribution of the AMOC term is larger in CMIP6 (supplementary material G), indicating that the difference in dependence on AMOC between CMIP5 and CMIP6 that we found is robust. Furthermore, we find that reducing the size of the smoothing window

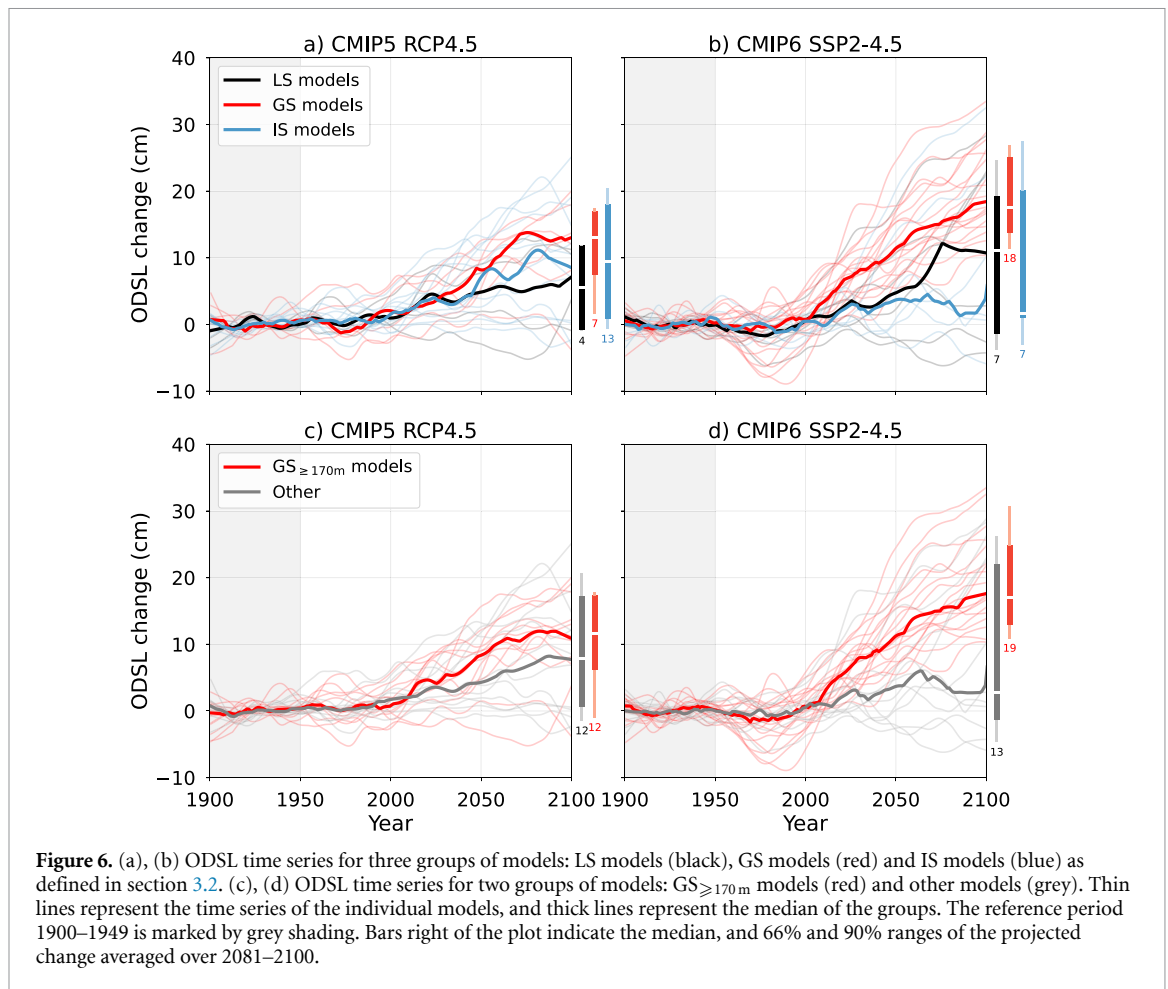


Figure 6. (a), (b) ODSL time series for three groups of models: LS models (black), GS models (red) and IS models (blue) as defined in section 3.2. (c), (d) ODSL time series for two groups of models: $GS_{\geq 170m}$ models (red) and other models (grey). Thin lines represent the time series of the individual models, and thick lines represent the median of the groups. The reference period 1900–1949 is marked by grey shading. Bars right of the plot indicate the median, and 66% and 90% ranges of the projected change averaged over 2081–2100.

reduces the relative importance of the AMOC in the regression model. This suggests that the short-term variability in ODSL seems to be influenced more by GSAT, whereas the longer-term variability is influenced more by the AMOC.

4.2. Deep ocean convection

In this section, we discuss the ODSL time series for the different categories of models explained in section 3.2. We focus on the results for intermediate emission scenario RCP4.5 / SSP2-4.5 as the results for the other scenarios are very similar (supplementary material H).

Figure 6 shows the ODSL time series, using different colours to represent the categories. Panels (a) and (b) show the categories based on the region where models experience the deepest mixed layer. We see that for both CMIP5 and CMIP6, models with the deepest mixed layer in the Greenland Sea project larger change in North Sea ODSL than models with a deeper mixed layer in one of the other regions. Moreover, we find that the relative number of models in the GS category increased in CMIP6.

The second categorisation uses a threshold depth of 170 m. For the Irminger Sea and Labrador Sea, we find that the ODSL projections from the group

of models exceeding this threshold are very similar to the projections from the models that have a shallower MLD. However, as presented in panel (c) and (d), models exceeding this threshold in the Greenland Sea show more change in ODSL than other models. Especially for the CMIP6 models, the difference between the Greenland Sea models and the others is notable. At the end of the century, the medians of the two categories differ more than 10 cm.

Combining the results from these four panels, we find that models with a deep mixed layer in the Greenland Sea during the period 1985–2004 project a larger rise of ODSL at the end of the century. This is the case for both CMIP5 and CMIP6, in all three scenarios. This suggests that the location of deep convection, characterised by a deep mixed layer, has an influence on North Sea ODSL. We find that more models have their deepest mixed layer in the Greenland Sea in CMIP6. Moreover, we find that in CMIP6, the number of models with the deepest mixed layer in the Greenland Sea increased, and the ratio of models exceeding the threshold of 170 m in the Greenland Sea to other models is larger in CMIP6 than in CMIP5. This suggests that the influence of deep ocean dynamics on ODSL in the North Sea might have increased between CMIP5 and CMIP6. A possible reason for

the increased number of models with a deeper mixed layer in the Greenland Sea could be a different representation of sea-ice in these models (Shu *et al* 2020).

To investigate whether we can draw conclusions about the real ocean from the modelled MLD, we compare CMIP output (figure 2) with a recent MLD climatology dataset (de Boyer Montégut *et al* 2004, De Boyer Montégut 2022). In accordance with earlier work (Sohail *et al* 2020, Heuzé 2021), we find that most CMIP models overestimate MLD by hundreds of meters in the three aforementioned regions. AMOC changes, however, impact ODSL locally through the associated change in heat and salt transport divergence, which then affects density and steric height (Menary and Wood 2018, Josey and Sinha 2022, Mecking and Drijfhout 2023). Steric changes at the eastern boundary of the North Atlantic that result from changes in heat and salt transport are transmitted to the North Sea via barotropic adjustment (Bingham and Hughes 2012, Dangendorf *et al* 2014). Here, we use MLD as a proxy for heat and salt transport divergence which is not available in many of the CMIP models. This is motivated by deep convection sites where MLD is maximal coinciding with maximum heat loss to the atmosphere and hence, maximum heat transport divergence (Lazier *et al* 2001). Therefore, it should be emphasised that the overestimation of MLD does not imply that CMIP models overestimate the link between AMOC and ODSL as well, as long as MLD qualitatively agrees with the main location of these transports. The observed MLD climatology shows that most deep water is formed in the Greenland Sea. This might imply that models in the GS category have a more realistic representation of the large-scale circulation in the North Atlantic and therefore of the sensitivity of ODSL to AMOC.

5. Conclusions

In this paper, we show that ODSL projections in the North Sea increased between CMIP5 and CMIP6. This difference is most pronounced in the low and intermediate emission scenarios. In addition to that, the inter-model spread increased between CMIP5 and CMIP6, in particular on the higher end of the uncertainty range.

We investigated processes that influence ODSL in the North Sea using linear regression models. We find that for CMIP6, neither GSAT nor GMTSL can reproduce ODSL projections based on a linear relation, whereas this was the case for CMIP5. Including the AMOC as an additional predictor enables us to reproduce long-term changes in ODSL for both ensembles. The results of the multilinear models

presented in this study should be interpreted with care because of the collinearity between the predictors. In order to validate our results, we repeated the analysis with different smoothing windows. We find a slight reduction in dependence on GSAT but a large increase in dependence on AMOC in CMIP6 compared to CMIP5. While the average AMOC strength did not change much between CMIP5 and CMIP6, the sensitivity to the AMOC increased leading to larger ODSL increase in CMIP6. This points to a difference in model dynamics between CMIP5 and CMIP6, and a more important role of the deep ocean.

Investigating this further, we find that the location of deep water formation in the North Atlantic potentially influences ODSL in the North Sea. We show that models with a deep mixed layer in the Greenland Sea project larger change in ODSL for both CMIP5 and CMIP6. The number of these models increased from CMIP5 to CMIP6, again pointing to a different sensitivity to larger scale processes in the ocean, and possibly explaining the ODSL difference between the two ensembles.

Data availability statement

The data that support the findings of this study are openly available at the following URL/DOI: <https://doi.org/10.5281/zenodo.5347692> (Le Bars 2021). Additional AMOC and MLD data is available at <https://zenodo.org/record/8005600> (Le Bars 2023). The code to produce those data is available on GitHub via https://github.com/dlebars/CMIP_SeaLevel. GSAT was downloaded from the KNMI Climate Explorer (<https://climexp.knmi.nl/start.cgi>). The code for the data analysis and creating the figures can be found on Github via: https://github.com/FrankaJes/ODSL_Analysis_Manuscript.

Acknowledgment

We would like to thank Céline Heuzé for providing us with mixed layer depth data. This publication was supported by the Knowledge Programme Sea Level Rise which received funding from the Dutch Ministry of Infrastructure and Water Management, the project RECEIPT (REmote Climate Effects and their Impact on European sustainability, Policy and Trade), which received funding from the European Union's Horizon 2020 research and innovation program (Grant No. 820712), and PROTECT, which received funding from the European Union's Horizon 2020 research and innovation program (Grant No. 869304). PROTECT contribution number 91.

ORCID iDs

Franka Jesse  <https://orcid.org/0009-0003-1928-6969>

Dewi Le Bars  <https://orcid.org/0000-0002-1175-4225>

References

- Bilbao R A, Gregory J M and Bouttes N 2015 Analysis of the regional pattern of sea level change due to ocean dynamics and density change for 1993–2009 in observations and CMIP5 AOGCMs *Clim. Dyn.* **45** 2647–66
- Bingham R and Hughes C 2012 Local diagnostics to estimate density-induced sea level variations over topography and along coastlines *J. Geophys. Res.* **117** C01013
- Bouttes N and Gregory J M 2014 Attribution of the spatial pattern of CO₂-forced sea level change to ocean surface flux changes *Environ. Res. Lett.* **9** 034004
- Bouttes N, Gregory J M, Kuhlbrodt T and Smith R 2014 The drivers of projected north Atlantic sea level change *Clim. Dyn.* **43** 1531–44
- Chen C, Liu W and Wang G 2019 Understanding the uncertainty in the 21st century dynamic sea level projections: the role of the amoc *Geophys. Res. Lett.* **46** 210–7
- Cleveland W S and Devlin S J 1988 Locally weighted regression: an approach to regression analysis by local fitting *J. Am. Stat. Assoc.* **83** 596–610
- Dangendorf S, Calafat F M, Arns A, Wahl T, Haigh I D and Jensen J 2014 Mean sea level variability in the north sea: processes and implications *J. Geophys. Res.* **119** 10
- Dangendorf S, Hay C, Calafat F M, Marcos M, Piecuch C G, Berk K and Jensen J 2019 Persistent acceleration in global sea-level rise since the 1960s *Nat. Clim. Change* **9** 705–10
- De Boyer Montégut C 2022 Mixed layer depth climatology computed with a density threshold criterion of 0.03 kg/m³ from 10 m depth value SEANOE [data set] (<https://doi.org/10.17882/91774>)
- de Boyer Montégut C, Madec G, Fischer A S, Lazar A and Iudicone D 2004 Mixed layer depth over the global ocean: an examination of profile data and a profile-based climatology *J. Geophys. Res.* **109** C12
- de Vries H, Katsman C and Drijfhout S 2014 Constructing scenarios of regional sea level change using global temperature pathways *Environ. Res. Lett.* **9** 115007
- Forster P M, Maycock A C, McKenna C M and Smith C J 2020 Latest climate models confirm need for urgent mitigation *Nat. Clim. Change* **10** 7–10
- Fox-Kemper B et al 2021 Ocean, Cryosphere and Sea Level Change In *Climate Change 2021: The Physical Science Basis (Contribution of Working Group I to the Sixth Assessment Report of the Intergovernmental Panel on Climate Change)* ed V Masson-Delmotte (Cambridge University Press) pp 1211–362
- Gill A and Niller P 1973 The theory of the seasonal variability in the ocean *Deep Sea Research and Oceanographic Abstracts* vol 20 (Elsevier) pp 141–77
- Gregory J M et al 2016 The flux-anomaly-forced model intercomparison project (FAFMIP) contribution to CMIP6: investigation of sea-level and ocean climate change in response to CO₂ forcing *Geosci. Model Dev.* **9** 3993–4017
- Gregory J M et al 2019 Concepts and terminology for sea level: mean, variability and change, both local and global *Surv. Geophys.* **40** 1251–89
- Harrison B J, Daron J D, Palmer M D and Weeks J H 2021 Future sea-level rise projections for tide gauge locations in south asia *Environ. Res. Commun.* **3** 115003
- Heuzé C 2017 North Atlantic deep water formation and amoc in CMIP6 models *Ocean Sci.* **13** 609–22
- Heuzé C 2021 Antarctic bottom water and north Atlantic deep water in CMIP6 models *Ocean Sci.* **17** 59–90
- Hinkel J, Church J A, Gregory J M, Lambert E, Le Cozannet G, Lowe J, McInnes K L, Nicholls R J, van Der Pol T D and van de Wal R 2019 Meeting user needs for sea level rise information: a decision analysis perspective *Earth's Future* **7** 320–37
- Hinkel J, Lincke D, Vafeidis A T, Perrette M, Nicholls R J, Tol R S, Marzeion B, Fettweis X, Ionescu C and Levermann A 2014 Coastal flood damage and adaptation costs under 21st century sea-level rise *Proc. Natl Acad. Sci.* **111** 3292–7
- Hobbs W, Palmer M D and Monselesan D 2016 An energy conservation analysis of ocean drift in the CMIP6 global coupled models *J. Clim.* **29** 1639–53
- Jesse F 2022 Ocean dynamic sea level projections during the 21st century along the dutch coast *Master's Thesis* Utrecht University The Netherlands
- Josey S A and Sinha B 2022 Subpolar Atlantic ocean mixed layer heat content variability is increasingly driven by an active ocean *Commun. Earth Environ.* **3** 111
- Katsman C A, Hazeleger W, Drijfhout S S, van Oldenborgh G J and Burgers G 2008 Climate scenarios of sea level rise for the northeast Atlantic ocean: a study including the effects of ocean dynamics and gravity changes induced by ice melt *Clim. Change* **91** 351–74
- Killworth P D 1983 Deep convection in the world ocean *Rev. Geophys.* **21** 1–26
- Kopp R E et al 2023 The Framework for Assessing Changes To Sea-level (FACTS) v1. 0: a platform for characterizing parametric and structural uncertainty in future global, relative, and extreme sea-level change *Geosci. Model Dev.* **16** 7461–89
- Lazier J, Pickart R and Rhines P 2001 Deep convection *Int. Geophys.* **77** 387–400
- Le Bars D 2021 Supporting data: 'receipt d7.3: future climate scenarios: sea level rise and sea ice extent *Zenodo* (<https://doi.org/10.5281/zenodo.5347692>)
- Le Bars D 2023 CMIP5 and CMIP6 post-processed amoc and mld data supporting jesse et al 2023 *Zenodo* (<https://doi.org/10.5281/zenodo.8005600>)
- Le Bras I A-A, Willis J and Fenty I 2023 The Atlantic meridional overturning circulation at 35 n from deep moorings, floats and satellite altimeter *Geophys. Res. Lett.* **50** e2022GL101931
- Lowe J A and Gregory J M 2006 Understanding projections of sea level rise in a hadley centre coupled climate model *J. Geophys. Res.* **111** C11014
- Lyu K, Zhang X and Church J A 2020 Regional dynamic sea level simulated in the CMIP5 and CMIP6 models: mean biases, future projections and their linkages *J. Clim.* **33** 6377–98
- McCarthy G D et al 2020 Sustainable observations of the amoc: methodology and technology *Rev. Geophys.* **58** e2019RG000654
- Mecking J V and Drijfhout S S 2023 The decrease in ocean heat transport in response to global warming *Nat. Clim. Change* **13** 1229–36
- Menary M B and Wood R A 2018 An anatomy of the projected north Atlantic warming hole in CMIP5 models *Clim. Dyn.* **50** 3063–80
- O'Neill B C, Kriegler E, Riahi K, Ebi K L, Hallegatte S, Carter T R, Mathur R and van Vuuren D P 2014 A new scenario framework for climate change research: the concept of shared socioeconomic pathways *Clim. Change* **122** 387–400
- Oppenheimer M et al 2019 Sea level rise and implications for low-lying islands, coasts and communities *Ipc Special Report on the Ocean and Cryosphere in a Changing Climate*, ed H-O Pörtner and D C Roberts (Intergovernmental Panel on Climate Change)
- Palmer M et al 2020 Exploring the drivers of global and local sea-level change over the 21st century and beyond *Earth's Future* **8** e2019EF001413
- Perrette M, Landerer F, Riva R, Frieler K and Meinshausen M 2013 A scaling approach to project regional sea level rise and its uncertainties *Earth Syst. Dyn.* **4** 11–29

- Shu Q, Wang Q, Song Z, Qiao F, Zhao J, Chu M and Li X 2020 Assessment of sea ice extent in CMIP6 with comparison to observations and CMIP5 *Geophys. Res. Lett.* **47** e2020GL087965
- Slangen A, Church J A, Agosta C, Fettweis X, Marzeion B and Richter K 2016 Anthropogenic forcing dominates global mean sea-level rise since 1970 *Nat. Clim. Change* **6** 701–5
- Sohail T, Gayen B and Hogg A M 2020 The dynamics of mixed layer deepening during open-ocean convection *J. Phys. Oceanogr.* **50** 1625–41
- Tibshirani R 1996 Regression shrinkage and selection via the lasso *J. R. Stat. Soc. B* **58** 267–88
- Van Vuuren D P *et al* 2011 The representative concentration pathways: an overview *Clim. Change* **109** 5–31
- Vousdoukas M I, Mentaschi L, Hinkel J, Ward P J, Mongelli I, Ciscar J-C and Feyen L 2020 Economic motivation for raising coastal flood defenses in Europe *Nat. Commun.* **11** 1–11
- Yuan J and Kopp R E 2021 Emulating ocean dynamic sea level by two-layer pattern scaling *J. Adv. Modeling Earth Syst.* **13** e2020MS002323